RSC Advances

PAPER

View Article Online
View Journal | View Issue

Cite this: *RSC Adv.*, 2025, **15**, 43645

A novel fluorescent nanoprobe based on DNA silver nanoclusters for the detection of DEQ

Yuxia Li,* Xingxing Liu, Baozhu Zhang * and Fengtao Gao

A novel fluorescent nanoprobe, constructed from silver nanoclusters templated by DNA, was developed for the detection of the cationic surfactant didecyl dimethyl ammonium chloride (DEQ). The presence of DEQ significantly diminishes the fluorescence intensity of the DNA-AgNCs. This reduction can be attributed to the negatively charged phosphate groups in the DNA-AgNCs, which, upon electrostatic adsorption, interact with the positively charged DEQ. This interaction leads to electron transfer from the DNA-AgNCs to DEQ, resulting in fluorescence quenching. The nanoprobe demonstrates a good linear range from 0 to 100 μM and a satisfactory detection limit of 2.0 μM. Moreover, the proposed nanoprobe has shown effective performance in DEQ detection in simulated wastewater.

Received 6th June 2025
Accepted 13th October 2025

DOI: 10.1039/d5ra04006j

rsc.li/rsc-advances

1 Introduction

In the context of rapid industrialization and urbanization, surfactants, a critical category of chemical raw materials, have found extensive applications in diverse domains such as washing, textiles, pharmaceuticals, pesticides, oil extraction, and food processing. However, environmental residues and accumulation of surfactants can potentially jeopardize ecosystems and human health, drawing considerable attention. Consequently, identifying surfactants in environmental samples has emerged as a pivotal research focus within the realm of analytical chemistry. In recent years, numerous studies have endeavored to develop and optimize techniques for detecting surfactants in environmental matrices, employing methodologies like online detection, spectroscopy, and electrochemical methods.[1–5] For example, ultraviolet-visible spectrophotometry and nanoparticle-assisted microextraction techniques have been utilized,[6,7] while some have even employed molecular dynamics simulations to accurately assess surfactant-micelle characteristics.[5] Therefore, the pursuit of efficient, precise, and expedient methods for surfactant determination is paramount for environmental preservation and pollution mitigation.

Silver nanoclusters templated by DNA (DNA-AgNCs) have garnered significant interest in biosensing and fluorescence imaging fields. These nanoclusters exhibit superior optical properties, including a high fluorescence quantum yield and robust photostability.[8–10] Additionally, their synthesis can be achieved through relatively straightforward procedures, controllable by the precise design of DNA sequences.[11–13] Notably, DNA-AgNCs offer unique advantages in the detection of DNA sequences, proteins, and other biomolecules, particularly in the development of innovative fluorescent probes and biosensors.[14–18] Furthermore, a conducting silver nanowire templated by DNA may allow the application of DNA for constructing functional circuits, and silver nanowires can also be utilized as sensitive optical detectors for biothiols, gas, DNA and other substances, and luminescent silver nanowires can be exploited for the visualization of genomic DNA sequences.[19]

Currently, both domestic and international research on the fluorescence method using DNA silver nanoclusters primarily concentrates on the synthesis of fluorescent probes, the characterization of their properties, and their application in specific fields. In the area of surfactant measurement, there is a limited amount of research based on the fluorescence method using DNA silver nanoclusters, despite some existing studies.[20] Furthermore, most extant measurement methods are plagued by issues such as complex operation, low sensitivity, and poor selectivity. For instance, the determination of non-ionic, cationic and anionic surfactants at low concentrations can often be carried out *via* high-performance liquid chromatography (HPLC), gas chromatography (GC), capillary electrophoresis (CE), or liquid chromatography-mass spectrometry and gas chromatography-mass spectrometry (LC-MS and GC-MS).[21] Although the detection limits are in the low μg L^{-1} or ng L^{-1} range, these methods can separate various isomers, homologues and oligomers of complex surfactant mixtures. However, there are also some steps that require effective enrichment and use toxic organic reagents, and some methods have low sensitivity,[22] or are subject to interference from other ionic surfactants and metal ions, requiring complex pretreatment, multiple process steps, or longer analysis times,[23,24] which pose a lot of difficulties in practical applications. Therefore, research on the determination of surfactants using the fluorescence method with DNA-stabilized silver nanoclusters not only advances the

Department of Chemistry and Chemical Engineering, Jinzhong University, Yuci 030619, P. R. China. E-mail: zhangbaozhu518@126.com; yxli_2004@163.com

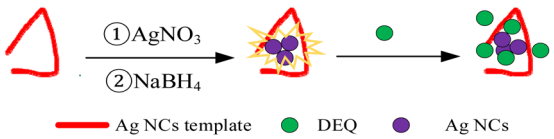

Scheme 1 Schematic diagram of the DEQ detection process.

development of this fluorescence method but also offers a novel technical approach for environmental surfactant monitoring.

Inspired by the above ideas, the cationic surfactant DEQ was detected using the DNA-AgNC fluorescence-quenching method for the first time. As depicted in Scheme 1, the DNA template for stabilizing AgNCs was designed, which contains more C bases for synthesis of DNA-AgNCs. The fluorescence of the DNA-AgNCs promptly decrease in the presence of DEQ due to electron transfer from the DNA-AgNCs to DEQ. The strategy has potential application value for detecting cationic surfactant content in the environment.

2 Experimental

2.1 Reagents and apparatus

Cationic surfactant didecyl dimethyl ammonium chloride (DEQ, 98%), non-ionic surfactant alkyl glycoside (APG-0810, 98%), fatty alcohol polyoxyethylene ether (AEO_7, 98%), anionic surfactant sodium laureth sulfate (AES, 98%), and the isomeric tridecanol phosphate (C13P, 98%) ester used in this work were obtained from the China Research Institute of Daily Chemical Industry (Shanxi, China). DNA was acquired from Yuanye Biotechnology Co. Ltd (Shanghai, China), with detailed specifications provided in SI Table S1. Sodium borohydride ($NaBH_4$, 98%) and silver nitrate ($AgNO_3$, 99.8%) were obtained from Aladdin Bio-Chem Technology Co. Ltd (Shanghai, China). All experiments were conducted using 20 mM phosphate buffer solution (PBS, pH 7.0) and ultrapure water (resistivity = 18.2 MΩ cm).

Fluorescence spectra were recorded on an FS5 spectrofluorometer (Edinburgh Instruments, UK) with excitation and emission slits set to 2 nm and 4 nm, respectively. Transmission electron microscopy (TEM) characterization was conducted using a Tecnai G2 F20 S-Twin microscope (FEI) at 200 kV acceleration voltage. XPS (X-ray photoelectron spectroscopy) analysis was performed with an ESCALAB 220i-XL system (VG Scientific) using Al Kα radiation (1486.6 eV). Fluorescence lifetimes were measured *via* time-correlated single-photon counting (TCSPC) methodology on an FS5 system (Edinburgh Instruments) with 405 nm excitation. Data analysis was performed using proprietary software provided by Edinburgh Instruments. When $\sum_{i=1}^{n} A_i = 1$, the average excited state lifetime is expressed by the equation $\tau_{avg} = \sum_{i=1}^{n} A_i \tau_i$. Each sample's spectrum was obtained by averaging three consecutive scans.

2.2 Preparation of silver nanoclusters

DNA-AgNCs were synthesized using a previously reported procedure in the literature.[25] In summary, $AgNO_3$ (18 μM) and DNA (3.0 μM) were sequentially introduced into PBS (20 mM, pH 7) with consistent stirring. The mixture was then incubated in the dark at 4 °C for 20 minutes. Subsequently, fresh $NaBH_4$ (18 μM) was added, and the solution was stirred for an additional minute before being shielded from light and stored at 4 °C for 1 hour. Then, the DNA-AgNCs were kept at 4 °C for further analysis.

2.3 Detection of DEQ

Subsequent additions of DEQ to the previously prepared DNA-AgNC mixture were carried out, with concentrations ranging from 0–200 μM. The fluorescence of the samples was detected at ambient temperature. In order to assess the specificity of the proposed DEQ probe, a range of DEQ analogues were evaluated, including the anionic surfactant sodium laureth sulfate (AES), the isomeric tridecanol phosphate ester C13P, and non-ionic surfactants APG-0810 and AEO_7. These measurements were conducted under conditions identical to those employed for the cationic surfactant DEQ.

2.4 Application of the proposed nanoprobe

DEQ in simulated domestic water samples was analyzed, with two simulated water samples being synthesized according to ref. 20. Sample 1 contains Na^+, K^+, Ba^{2+} and Cr^{3+}, and Sample 2 contains NH^{4+}, Zn^{2+}, Mg^{2+} and K^+. The concentration of each ion is 0.2 μM and the DEQ solution was at 40 μM. Following the experimental steps employed for DEQ detection, the fluorescence quenching degree and spiked recovery rate were calculated.

3 Results and discussion

3.1 Optical characterization of DNA-AgNCs

The photophysical properties of DNA-templated silver nanoclusters (AgNCs) exhibit a strong dependence on the structural features of their DNA templates, particularly the base sequence composition and secondary structure conformation.[26,27] Consequently, two specific DNA templates, D-DNA and D1-DNA, were meticulously designed for this study. The sequences of these templates can be found in SI Table S1. D1-DNA is derived from D-DNA, where the content of CGAA has been increased. Fig. 1 presents the photophysical properties of the D-DNA-

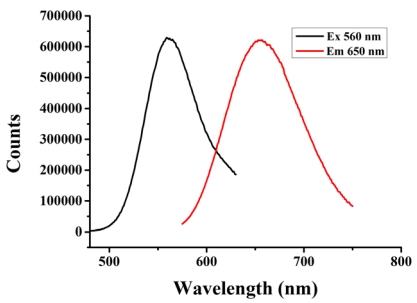

Fig. 1 The excitation (black) and emission (red) spectra of D-DNA-AgNCs.

AgNCs. The fluorescence profile shows well-defined excitation and emission maxima at 560 nm and 650 nm, respectively (black and red curves), indicating the characteristic optical transitions of the synthesized AgNCs. Similar spectroscopic characterization was performed for D1-DNA-AgNCs, with the fluorescence spectra displaying well-defined excitation (605 nm) and emission (680 nm) bands (see SI Fig. S1).

Furthermore, the UV-Vis absorption spectra of the D-DNA-AgNCs were analyzed at varying concentrations of DEQ. In every curve of SI Fig. S2, two peaks are discernible: a peak at 430 nm, which is characteristic of the plasmon absorption band of Ag nanoparticles, and a peak at 565 nm, which corresponds to the absorption band of AgNCs.[28] This indicates the presence of Ag nanoparticles within the D-DNA-AgNCs. As the concentration of DEQ increases, there is a noticeable gradual decrease in absorption.

The temporal stability of the fluorescence intensity of the D-DNA-AgNCs and D1-DNA-AgNCs was systematically evaluated, as probe stability critically influences detection performance. As shown in SI Fig. S3, the D-DNA-AgNCs exhibit distinct stability characteristics: the fluorescence intensity stabilizes after 2.5 hours, remains constant for approximately 2.0 hours, and then gradually decreases. In contrast, the D1-DNA-AgNCs demonstrate a continuous decline in fluorescence intensity over time. These results clearly indicate that the D-DNA-AgNCs possess superior stability compared to their D1-DNA-AgNC counterparts.

The fluorescence emission efficiencies of the D-DNA-AgNC and D1-DNA-AgNC probes were evaluated by measuring their quantum yields (QYs). As illustrated in SI Fig. S4, the QY values were determined to be 30.05% and 20.30% for D-DNA-AgNCs and D1-DNA-AgNCs, respectively.

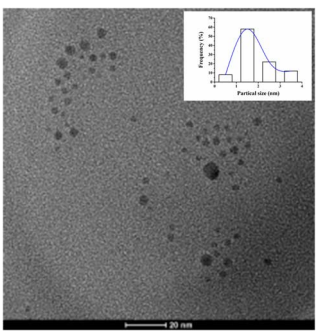

Fig. 2 TEM micrograph of D-DNA-AgNCs along with their size distribution histogram (inset).

3.2 Characteristics of D-DNA-AgNC

Transmission electron microscopy (TEM) was employed to investigate the structural properties of the D-DNA-AgNCs. Fig. 2 reveals a homogeneous dispersion of these nanoclusters, with an average particle size of 2 nm, aligning with reported dimensions for metal NCs smaller than 2 nm.[29] The size distribution was quantified through Lorentzian fitting of the corresponding histogram. The oxidation states of silver in the D-DNA-AgNCs were verified *via* XPS spectroscopy. The Ag 3d region (Fig. 3B) exhibits two peaks at binding energies of 368.25 eV ($3d_{5/2}$) and 374.20 eV ($3d_{3/2}$), corresponding to Ag(I) and Ag(0) species, respectively.[30,31] The elemental composition, as determined by XPS (Fig. 3A), reveals characteristic peaks corresponding to P, B, C, N, Na, and O.

3.3 Optimizing assay conditions

3.3.1 Influence of DEQ on different DNA-AgNCs. The fluorescence characteristics of silver nanoclusters synthesized using various DNA templates exhibit variations, attributable to the differences in base sequences and secondary structures of the DNA templates.[32,33] The fluorescence intensities of the D-DNA-AgNCs and D1-DNA-AgNCs upon the addition of 110 μM DEQ were assessed. As shown in SI Fig. S5, both fluorescence intensities decrease promptly upon DEQ addition. Notably, the relative fluorescence intensity (F/F_0, where F and F_0 represent the fluorescence intensities of the AgNCs with and without the addition of 110 μM DEQ, respectively) of the D-DNA-AgNCs exhibits the most pronounced reduction, with F/F_0 falling below 0.0086. Consequently, D-DNA-AgNCs are selected as the superior candidate for subsequent experiments.

3.3.2 Optimization of fluorescence quenching concentration. The optimal concentration for DEQ fluorescence quenching was ascertained, as illustrated in SI Fig. S6. With an increase in the DEQ concentration, there is a corresponding gradual decrease in the fluorescence intensity of the D-DNA-AgNCs. When the DEQ concentration reaches 100 μM, the fluorescence intensity attains its minimum value and subsequently

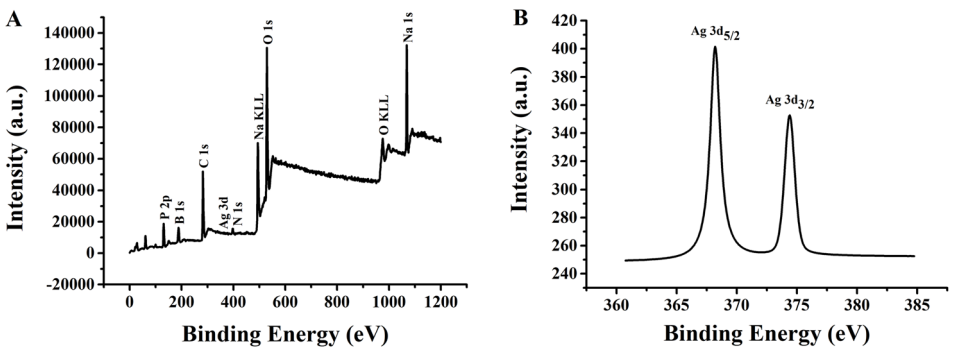

Fig. 3 (A) XPS spectrum of D-DNA-AgNCs. (B) Ag 3d region of XPS spectrum of D-DNA-AgNCs.

remains stable. Thus, the optimal fluorescence quenching concentration of D-DNA-AgNCs for detecting DEQ is 100 μM.

3.3.3 Optimization of reaction time. The fluorescence quenching time between the D-DNA-AgNCs and 100 μM DEQ was ascertained in an effort to enhance the detection capability of the developed nanoprobe toward DEQ. SI Fig. S7 demonstrates the fluorescence intensity of the fluorescent probe decreases sharply at the beginning, and there is not much change in the fluorescence intensity after 10 min. That is, the time required for DEQ to quench the fluorescence of the D-DNA-AgNC fluorescent probe is 10 min.

3.4 Assay of DEQ

The D-DNA-AgNCs' fluorescence emissions were recorded over a DEQ concentration range of 0–100 μM. As shown in Fig. 4A and B, the fluorescence signal progressively weakened with higher DEQ concentrations, showing a linear correlation (R^2 = 0.9297) described by $F = 191\,036.4 - 1660.8C_{DEQ}$. The detection limit was determined to be 2.0 μM using the $3\sigma_0/k$ method (where σ_0 represents the background signal variability and k denotes the calibration curve slope). As shown in Table S3, the LOD of the proposed nanoprobe is not superior to that of a reported sensor for detecting cetyltrimethylammonium bromide,[20] but it is superior to other probes.[34,35] Although the LOD of this method cannot be evaluated under wastewater discharge conditions due to the difficulty of obtaining suitable standards for cationic surfactants, it provided a novel method for detecting cationic surfactant content. The sensitivity will be gradually improved in the future.

The quenching process was examined by monitoring the lifetime changes of the D-DNA-AgNCs (650 nm emission) upon DEQ addition. The lifetime of the D-DNA-AgNCs also shows an upward trend with rising DEQ concentrations, characteristic of dynamic quenching (SI Fig. S8). The fluorescence transient of the D-DNA-AgNCs demonstrates a monoexponential time constant (SI Table S2).

3.5 Interference study on the nanoprobe's DEQ recognition

Selectivity is a critical parameter for a high-quality fluorescent probe. This study investigates the selectivity towards the cationic surfactant DEQ and other types of surfactants, including nonionic surfactants APG0810 and AEO_7, as well as the anionic surfactants isomeric tridecyl phosphate ester (C13P) and sodium laureth sulfate (AES), at concentrations of 100 μM. As illustrated in Fig. 5, a significant relative fluorescence reduction occurs in the presence of 100 μM DEQ. In contrast, the presence of other surfactant types results in only a negligible decrease. This differential response may be attributed to the presence of negatively charged phosphate groups in the DNA-AgNCs. These findings suggest that the proposed probe exhibits high selectivity for assays of the cationic surfactant DEQ.

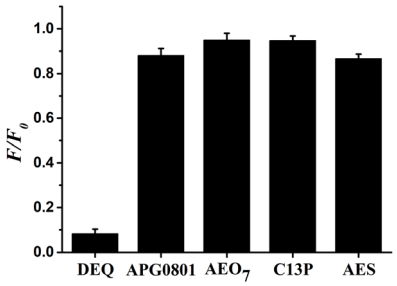

Fig. 5 Selectivity of the DEQ detection system. Error bars represent the standard deviation of three repeated experiments.

3.6 Application of nanoprobe for detecting DEQ in industrial waste water

Under the experimentally determined optimal conditions, two simulated samples are synthesized, with synthesized Sample 1 containing Na^+, Cr^{3+}, Ba^{2+} and K^+, and synthesized Sample 2 containing NH_4^+, Zn^{2+}, Mg^{2+} and K^+. The two simulated samples are separately added to the synthesized DNA-AgNCs, and then 40 μM of DEQ. The results show that the quenching effect of the added samples is basically consistent with the quenching effect without adding samples. As illustrated in Table 1, the recoveries of DEQ using this method were 100.3% and 104.6%, with relative standard deviations of 0.40 and 0.32, respectively. These results suggest that this nanoprobe is not only reliable but also

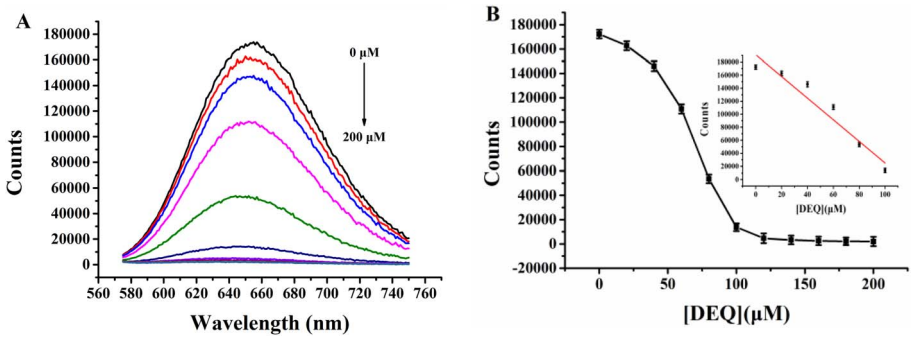

Fig. 4 (A) Fluorescence emission spectra of D-DNA-AgNCs in the presence of DEQ (0–200 μM). (B) DEQ-concentration-dependent changes of fluorescence intensity at 650 nm. (Inset) Linear relationship between F_{650} nm and DEQ concentration (0–100 μM). Error bars represent the standard deviation of three repeated experiments.

Table 1 The concentration of DEQ in simulated samples measured with the proposed probe ($N = 3$)

Samples	Spiked (μM)	Measured (μM), mean[a] ± SD[b]	Recovery (%), RSD (%)
1	40	40.11 ± 0.16	100.3%, 0.40
2	40	40.23 ± 0.13	104.6%, 0.32

[a] The mean of three determinations. [b] Standard deviation. RSD = relative standard deviation.

exhibits high precision for the determination of DEQ in industrial wastewater.

3.7 Mechanism study

To verify if the mechanism involved electron transfer caused by electrostatic adsorption, the zeta potential of the D-DNA-AgNCs was measured in the presence of different concentrations of DEQ. As shown in SI Fig. S9, the zeta potential gradually increased with increasing DEQ concentrations. DNA-AgNCs have an anionic phosphate backbone and DEQ is a cationic surfactant.

The zeta potential of the DNA-AgNCs is −10.47 mV at first with DNA-AgNCs carrying negative charge. The zeta potential gradually increases as DEQ continues to be added, due to electrostatic adsorption. In addition, the alkyl chain length of DEQ may affect the adsorption mode and the quenching efficiency. DEQ becomes difficult to dissolve in water if the alkyl chain of DEQ is lengthened. Therefore, the possibility of electrostatic adsorption occurring decreases, such that the DNA-AgNCs cannot be quenched.

4 Conclusions

This study establishes a method for detecting the cationic surfactant DEQ using the fluorescence quenching method with DNA-stabilized silver nanoclusters. This method is only applicable to cationic surfactants and cannot be effectively applied to the determination of anionic surfactants and nonionic surfactants. The method has high sensitivity, strong selectivity, low cost, and environmental friendliness, and has been applied to the detection of simulated environmental wastewater samples. The research results provide an effective method for the detection of cationic surfactants in environmental samples.

Conflicts of interest

There are no conflicts to declare.

Data availability

The data supporting this article have been included within the article and as part of the supplementary information (SI). Supplementary information: the messages of the oligonucleotides; the lifetimes of D-DNA-Ag NCs; the LOD of some of cationic surfactants; the excitation and emission spectra of D1-DNA-AgNCs; the UV-Vis absorption spectra of D-DNA-Ag NCs studies; the temporal stability of D-DNA-Ag NCs and D1-DNA-Ag NCs; the quantum yields (QY) of D-DNA-AgNCs and D1-DNA-AgNCs; the relative fluorescence intensity (F/F_0) of different DNA-AgNCs; optimizing assay conditions; the fluorescence lifetimes of D-DNA-Ag NCs; the change of the zeta potential of D-DNA-Ag NCs against the increasing DEQ concentration. See DOI: https://doi.org/10.1039/d5ra04006j.

Acknowledgements

This work was supported by the Important Research and Development Plan of Shanxi Province (201803D121036), the Startup Foundation of Doctors of Jinzhong University (23E00345) and Shanxi Province New Multi-functional Glass Technology Innovation Center.

Notes and references

1 L. Wei, Y. C. Dai, Q. J. Xu, Y. H. Ju and H. H. Ge, *Online Determination of Anionic Surfactant in Environmental Water PESE*, 2013, pp. 1113–1116.
2 Y. H. Liu, H. W. Zhan and W. X. Ma, *Asian J. Chem.*, 2013, **25**, 2736–2738.
3 Z. P. Wei, S. Bilbulian, J. N. Li, P. Ratnesh and E. O'Connor, *J. Sep. Sci.*, 2015, **38**, 1318–1325.
4 T. D. Smirnova, E. A. Alyabeva and N. A. Yurasov, *J. Anal. Chem.*, 2024, **79**, 628–634.
5 S. Faramarzi, B. Bonnett, C. Scaggs, A. Hoffmaster and D. Grodi, *Langmuir*, 2017, **33**, 9934–9943.
6 Y. Y. Man, *Groundwater*, 2018, **40**, 74.
7 N. Rahimian, J. Feizy and Z. Eshaghi, *J. Chromatogr. Sci.*, 2024, **62**, 995–1006.
8 Y. Teng, H. Tateishi Karimata, T. Tsuruoka and N. Sugimoto, *Molecules*, 2018, **23**, 1–12.
9 J. Peng, Y. Shao, L. L. Liu, L. H. Zhang, W. S. Fu and H. Liu, *Nanotechnology*, 2014, **25**, 235501.
10 D. Y. Lu, J. Li, X. W. Wang, W. W. Guo and E. K. Wang, *J. Anal. Chem.*, 2019, **91**, 2050–2057.
11 X. M. Miao, Z. Y. Cheng, H. Y. Ma, Z. B. Li and N. Xue, *J. Anal. Chem.*, 2018, **90**, 1098–1103.
12 J. M. Obliosca, C. Liu and H. C. Yeh, *Nanoscale*, 2013, **5**, 8443–8461.
13 Y. S. Ang, W. W. E. Woon and L.-Y. L. Yung, *Nucleic Acids Res.*, 2018, **46**, 6974–6982.
14 C. Wang, K. Y. Xing, G. G. Zhang, M. F. Yuan and S. L. Xu, *Food Chem.*, 2019, **281**, 91–96.
15 Z. R. Xiao, D. H. Huang, M. M. Bian, Y. L. Yuan and J. F. Nie, *Chem. Res. Chin. Univ.*, 2020, **41**, 102–110.
16 J. Y. Wang, Z. Liu, Q. Zhang, C. Y. Sun and H. X. Li, *Chem. Res. Chin. Univ.*, 2022, **43**, 20220010–20220015.
17 H. C. Yadavalli, S. Park, Y. Kim, R. Nagda and T. Kim, *Small*, 2024, **20**, 856–863.

18 Y. T. Jiang, Z. Z. Guo, M. Y. Wang, J. J. Cui and P. Miao, *Nanoscale*, 2022, **14**, 612–616.
19 Q. Ma, M. Chinappi, A. Douaki, Y. Zou, H. Jin, E. Descrovi, R. Krahne, R. P. Zaccaria, R. Marotta, W. Wang, D. Cojoc, K. kołątaj, G. Acuna, S. Jin and D. Garoli, *Nanoscale*, 2025, **17**, 16342–16348.
20 C. Liu, X. X. Zhu, S. Y. Yang, X. Lin and W. Chen, *CRAJ*, 2020, **32**, 1716–1719.
21 C. Vogt and K. Heinig, *J. Anal. Chem.*, 1999, **363**, 612–618.
22 Y. Yokoyama, H. Kubo and H. Sato, *Talanta*, 2008, **77**, 667–672.
23 M. Kamaya, J. Takahashi and K. Nagashima, *Microchim. Acta*, 2004, **144**, 35–39.
24 A. K. Trofimchuk and Y. B. Tarasova, *J. Anal. Chem.*, 2004, **59**, 114–118.
25 B. Z. Zhang and C. Y. Wei, *J. Anal. Bioanal. Chem.*, 2020, **412**, 2529–2536.
26 E. G. Gwinn, P. O'Neill, A. J. Guerrero, D. Bouwmeester and D. K. Fygenson, *Adv. Mater.*, 2008, **20**, 279–283.
27 K. Loo, N. Degtyareva, J. Park, B. Sengupta, M. Reddish, C. C. Rogers, A. Bryant and J. T. Petty, *J. Phys. Chem. B*, 2010, **114**, 4320–4326.
28 J. Xu and C. Wei, *Biosens. Bioelectron.*, 2017, **87**, 422–427.
29 X.-R. Song, N. Goswami, H.-H. Yang and J. Xie, *Analyst*, 2016, **141**, 3126–3140.
30 K. R. Krishnadas, A. Ghosh, A. Baksi, I. Chakraborty, G. Natarajan and T. Pradeep, *J. Am. Chem. Soc.*, 2016, **138**, 140–148.
31 Q. Zhou, Y. Lin, M. Xu, Z. Gao, H. Yang and D. Tang, *J. Anal. Chem.*, 2016, **88**, 8886–8892.
32 E. G. Gwinn, P. O'Neill, A. J. Guerrero, D. Bouwmeester and D. K. Fygenson, *Adv. Mater.*, 2008, **20**, 279–283.
33 K. Loo, N. Degtyareva, J. Park, B. Sengupta, M. Reddish, C. C. Rogers, A. Bryant and J. T. Petty, *J. Phys. Chem. B*, 2010, **114**, 4320–4326.
34 P. Fernandez, A. C. Alder, M. J.-F. Suter and W. Giger, *J. Anal. Chem.*, 1996, **68**, 921–929.
35 K. Kümmerer, A. Eitel, U. Braun, P. Hubner, F. Daschner, G. Mas-cart, M. Milandri, F. Reinthaler and J. Verhoef, *J. Chromatogr. A*, 1997, **774**, 281–286.